Bioorganic & Medicinal Chemistry 20 (2012) 903–909

Contents lists available at SciVerse ScienceDirect

Bioorganic & Medicinal Chemistry

journal homepage: www.elsevier.com/locate/bmc

Design, synthesis, biological evaluation and molecular modeling of 1,3,4-oxadiazoline analogs of combretastatin-A4 as novel antitubulin agents

Yang Hu, Xiang Lu, Ke Chen, Ru Yan, Qing-Shan Li, Hai-Liang Zhu *

State Key Laboratory of Pharmaceutical Biotechnology, Nanjing University, Nanjing 210093, People's Republic of China

ARTICLE INFO

Article history:
Received 5 October 2011
Revised 25 November 2011
Accepted 25 November 2011
Available online 3 December 2011

Keywords:
Combretastatin-A4
1,3,4-Oxadiazoline
Tubulin inhibitors
Molecular docking

ABSTRACT

A total of 20 novel 1,3,4-oxadiazoline analogs (**6a–6t**) of combretastatin A-4 with naphthalene ring were designed, synthesized, and evaluated for biological activities as potential tubulin polymerization inhibitors. Among these compounds, **6n** showed the most potent antiproliferative activities against multiple cancer cell lines and retained the microtubule disrupting effects. Docking simulation was performed to insert compound **6n** into the crystal structure of tubulin to determine the probable binding model. These results indicated oxadiazoline compounds bearing the naphthyl moiety are promising tubulin inhibitors.

1. Introduction

Two decades ago, combretastatins, as natural antimitotic agents, were isolated from the bark of the South African tree *Combretum caffrum*.[1,2] Among these compounds, combretastatin A-4 (CA-4, Fig. 1a) possessed the most potent and interesting antitumor activity. And early work showed it inhibited tubulin polymerization and the proliferation of murine and human cancer cells.[3,4] Since it is such a simple structure bringing only two aromatic rings linked by a double bond in the *cis* configuration, hundreds of Combretastatin derivatives have been synthesized and further studied as tubulin inhibitors.

For the sake of simplicity, here the molecule is subdivided into three main parts (ring A, ring B, and the bridge; Fig. 1b). Various structural modifications to CA-4 have been reported. The structural modifications to the double bond are topics of most concern. It is believed that the olefinic bond plays a more constitutive role than a binding role during the biological interaction; it allows placement of the aromatic rings at an appropriate distance and gives the molecule the right dihedral. Among the modifications, the replacement with five-membered rings is the promising target. Imizadoles, chalcones, 1,3-oxazole, pyrazole, triazoles, furazan, 2(5*H*)-furanone, diaryloxazolones, 2-cyclopentenl-one, 4,5-dihydroisoxazole, 2, 3-dihydrothiophene and arylcoumarin have been synthesized to date.[5–13] Most of these retain both cytotoxic and antitubulin activity. Indeed, a number of compounds were found to be slightly more potent than Combretastatin itself.[6] The structural modifications to ring A had received very little attention. Most combretastatin derivatives retained the trimethoxybenzene moiety. But some excellent work of Keira's group showed no necessity of the three methoxyl groups in ring A for biological activity.[14] Besides, some SAR showed modification of the trimethoxybenzene with groups of higher lipophilicity could lead to decreased cytotoxicity and increased antitubulin activity.[15] Some previous results implied that the naphthalene ring was a good surrogate for the trimethoxyphenyl[16] to fix in the hydrophobic pocket of the tubulin. Ring B has received greater

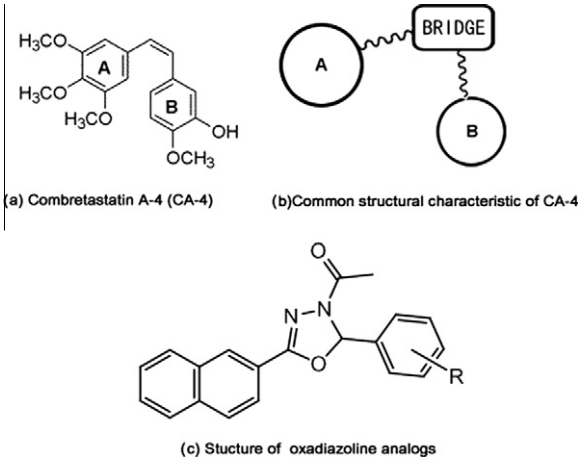

Figure 1. Structure of CA-4 and oxadiazoline analogs and common structural characteristic of CA-4.

* Corresponding author. Tel./fax: +86 25 83592672.
E-mail address: zhuhl@nju.edu.cn (H.-L. Zhu).

0968-0896/$ - see front matter © 2011 Elsevier Ltd. All rights reserved.
doi:10.1016/j.bmc.2011.11.057

attention from medicinal chemists. Substituents on Ring B of the combretastatins are the key atoms which interact with tubulin and inhibit its assembly.

A new series of 2-(2′-naphthyl)-5-phenyl-1,3,4-oxadiazoline analogs (Fig. 1c) were designed to retain the geometric features of CA-4. Compared to other five-membered rings, the oxadiazoline moiety should provide an optimal conformational geometry for interaction with the colchicine binding site.[5,17,18] Also our lab had reported 1,3,4-oxadiazole derivatives show broad spectrum of bioactivities, which implied the oxadiazoline moiety was promising skeleton of anticancer agents.[19] The net effect is an increase in the polarity of the molecule, which should enhance water solubility. And some previous results imply that the naphthalene ring, which has higher lipophilicity can fix in the hydrophobic pocket of the tubulin better.[20]

These oxadiazoline analogs were synthesized and evaluated for biological activities. Docking simulation was also performed using X-ray crystallographic structure of the tubulin to explore the binding modes of the synthetic compounds at the active site of the enzyme.

2. Results and discussion

2.1. Chemistry

The synthetic route for 20 oxadiazoline analogs **6a–6t** is outlined in Scheme 1. These analogs were synthesized by adapting a procedure reported by Ali, Amer, and Abdel-Rahman.[21] The key hydrazide intermediates **3** were prepared in two steps. Esterification of the carboxylic acids **1** with ethanol and concentrated sulfuric acid afforded the corresponding esters **2**. The naphthyl hydrazides **3** were obtained by reaction of esters **2** with 85% hydrazine monohydrate in ethanol. The reaction of a hydrazide **3** with aldehyde **4** in reflux with water and glacial acetic acid in ethanol for 5 h produced the hydrazone intermediate **5**. The target compounds **6a–6t** were obtained by refluxing an appropriate hydrazone intermediate in acetic anhydride for 1 h. All of the synthetic compounds gave satisfactory analytical and spectroscopic data, which were in full accordance with their depicted structures.

Table 1
Inhibition of cancer cells proliferation and tubulin polymerization by compounds **6a–6t**

Compound	IC_{50} ± SD (μg/mL)			IC_{50} ± SD (μM)
	HepG2[a]	MCF-7[b]	B16-F10[c]	Tubulin[d]
6a	2.11 ± 0.15	2.43 ± 0.27	2.57 ± 0.10	21.2 ± 1.3
6b	3.60 ± 0.38	7.35 ± 0.64	6.86 ± 0.91	105.2 ± 10.2
6c	3.98 ± 0.21	5.49 ± 0.73	6.98 ± 0.54	51.5 ± 2.7
6d	1.68 ± 0.11	2.34 ± 0.19	2.36 ± 0.13	19.4 ± 1.4
6e	2.08 ± 0.17	5.07 ± 0.36	4.68 ± 0.33	33.8 ± 2.4
6f	4.32 ± 0.22	2.36 ± 0.16	4.93 ± 0.39	51.4 ± 2.6
6g	1.88 ± 0.13	2.63 ± 0.25	2.48 ± 0.13	12.7 ± 1.7
6h	3.36 ± 0.24	3.44 ± 0.54	6.05 ± 0.45	48.1 ± 5.6
6i	1.86 ± 0.10	1.98 ± 0.29	1.61 ± 0.13	9.2 ± 2.0
6j	1.82 ± 0.33	3.02 ± 0.43	4.65 ± 0.48	28.1 ± 1.9
6k	12.32 ± 2.3	18.20 ± 2.1	9.01 ± 0.63	140.5 ± 9.1
6l	8.10 ± 0.51	7.59 ± 0.44	9.32 ± 1.03	103.2 ± 9.3
6m	1.84 ± 0.19	2.12 ± 0.37	2.58 ± 0.32	27.1 ± 2.0
6n	0.85 ± 0.06	1.01 ± 0.11	1.56 ± 0.20	4.3 ± 0.7
6o	5.26 ± 0.29	6.02 ± 0.72	7.18 ± 0.69	53.8 ± 1.5
6p	2.86 ± 0.19	2.61 ± 0.06	3.06 ± 0.29	20.1 ± 3.8
6q	2.17 ± 0.27	2.56 ± 0.36	2.97 ± 0.20	22.8 ± 1.3
6r	2.26 ± 0.15	2.90 ± 0.17	3.85 ± 0.31	30.5 ± 2.6
6s	6.82 ± 0.58	7.98 ± 0.42	8.56 ± 0.47	51.9 ± 4.4
6t	3.38 ± 0.08	5.49 ± 0.32	8.08 ± 0.73	58.2 ± 6.12
CA-4	0.54 ± 0.02	0.48 ± 0.02	0.75 ± 0.04	2.9 ± 0.2

[a] Inhibition of the growth of HepG2 cell lines.
[b] Inhibition of the growth of MCF-7 cell lines.
[c] Inhibition of the growth of B16-F10 cell lines.
[d] Inhibition of tubulin polymerization.

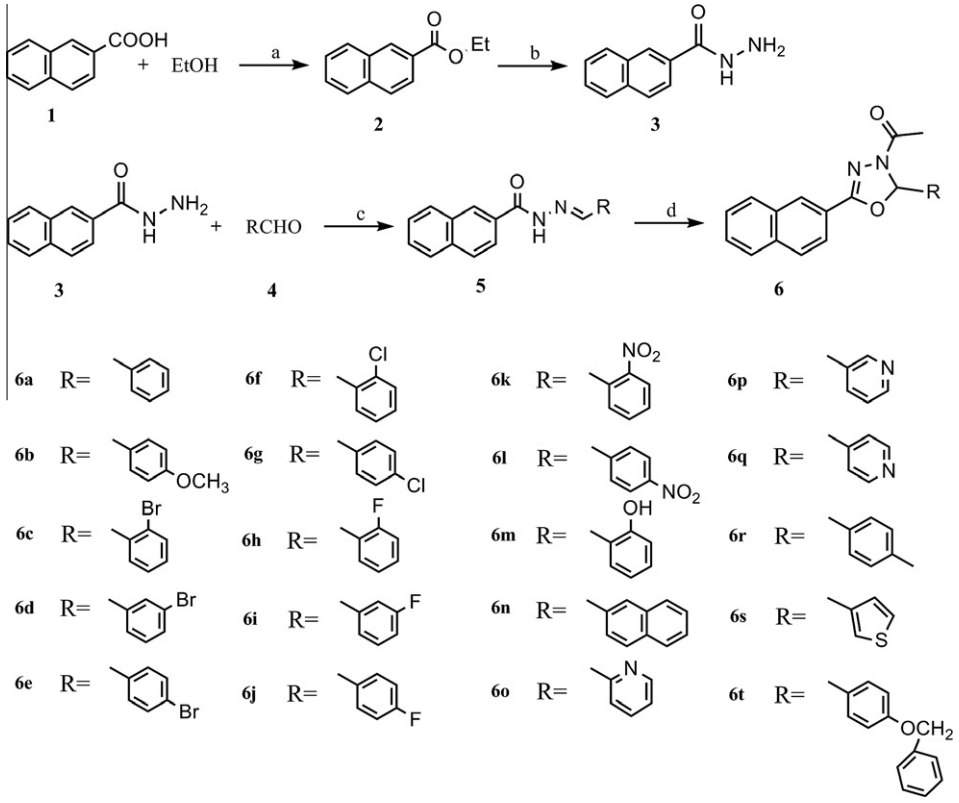

Scheme 1. Synthesis of compounds **6a–6t**. Reagents and conditions: (a) H_2SO_4, reflux, 8–12 h; (b) NH_2NH_2–H_2O (85%), ethanol, reflux, 8–12 h; (c) ethanol, water, acetic acid, reflux, 5 h; (d) acetic anhydride, reflux, 1 h.

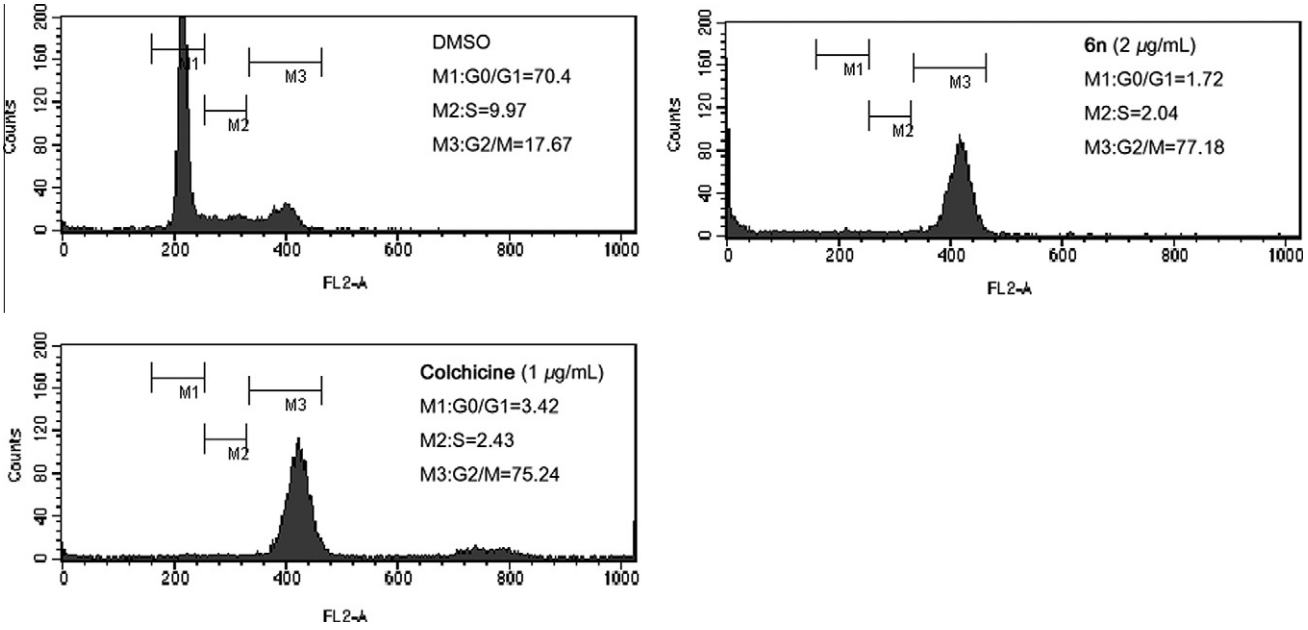

Figure 2. Effects of compound **6n** on cell cycle progression of B16-F10 cells were determined by flow cytometry analysis. B16-F10 cells were treated with 6n for 24 h. The percentage of cells in each cycle phase was indicated.

2.2. Antiproliferative effects against cancer cells

The antiproliferative effects of the 20 compounds were evaluated in HepG2, MCF-7 and B16-F10 cells and the IC_{50} values determined. The results were summarized in Table 1. A number of oxadiazoline compounds bearing the same naphthyl moiety showed remarkable effects on antiproliferative activities. The results reveal several interesting points including the broad range of potencies in this series.

Compounds **6b–6j** with *para* substituted on phenyl ring exhibited antiproliferative activities in order of Cl > F > Br > Me. And the *ortho* and *meta* substituted showed the similar order. Moreover, compound **6b** with methoxyl group showed poor activity, suggesting that methoxyl group be not critical for the potent activity in oxadiazoline analogs. Besides, introduction of *ortho*-hydroxy to phenyl ring gave compound **6m** significant activity, while that of *ortho*-nitryl brought reduced activity.

In an attempt to improve inhibitory activity of **6a**, its phenyl ring was replaced with a pyridine group (**6o–6q**). This resulted in a slight decrease in potency. It demonstrated that benzene ring was favorable for the potent activity which might explain compound **6n** with naphthyl moiety displays most potent activity.

The results showed that *meta* electron-withdrawing and *ortho* electron-donating groups in aromatic ring could enhance the activity of compounds. It could be a promising lead for the further development of novel tubulin inhibition agents.

2.3. Tubulin polymerization inhibition

After these results, we checked the abilities of the synthesized compounds in inhibiting the polymerization of tubulin. As shown in Table 1, IC_{50} against tubulin polymerization corresponds with IC_{50} value against cancer cells in general. Compounds **6i** and **6n**

Table 2
Predicted binding free energy (kcal/mol) and the experimental activity (pIC_{50}, $-\log IC_{50}$) against tubulin

Compound	ΔG (kcal/mol)	pIC_{50}[a]
6a	−17.39	4.17
6b	−13.56	3.51
6c	−13.58	3.88
6d	−16.04	4.30
6e	−15.80	4.06
6f	−16.00	3.83
6g	−15.85	4.44
6h	−15.21	3.84
6i	−17.18	4.55
6j	−16.68	4.07
6k	−13.80	3.40
6l	−13.42	3.54
6m	−17.02	4.08
6n	−17.40	4.93
6o	−15.71	3.77
6p	−15.63	4.19
6q	−16.35	4.14
6r	−15.81	4.03
6s	−14.15	3.79
6t	−15.93	3.86

[a] pIC_{50} represents $-\log IC_{50}{}^{tubulin}$.

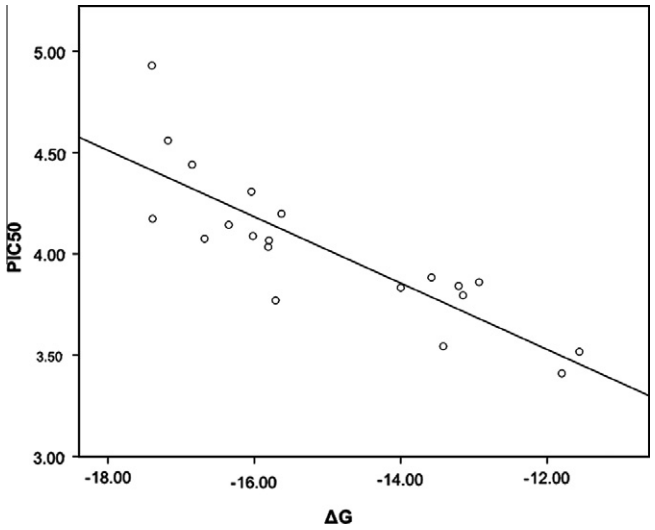

Figure 3. Correlation between the binding free energy (ΔG, kcal/mol) of compounds with tubulin and the experimental activities ($-\log IC_{50}$).

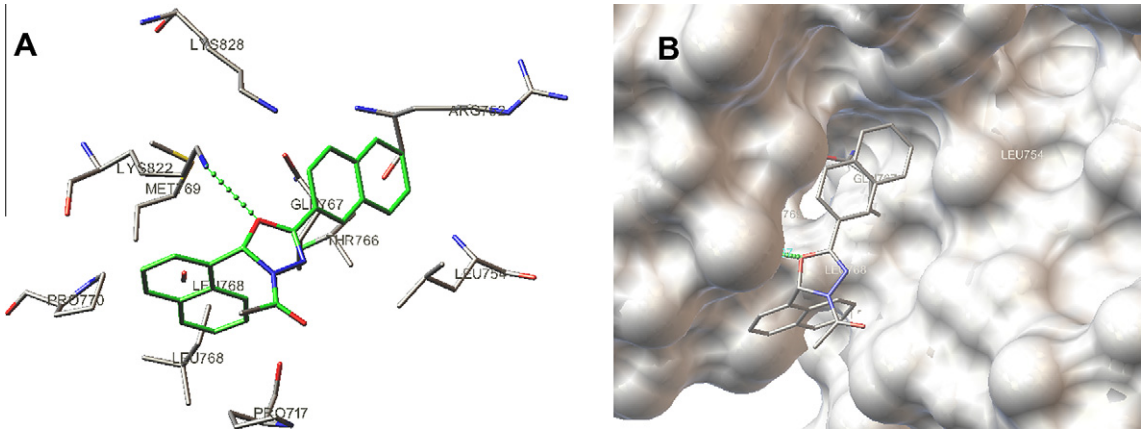

Figure 4. (A) Binding mode of compound **6n** (colored by atom: carbons: green; oxygens: red) with tubulin (entry 1SA0 in the Protein Data Bank). The dotted lines show the hydrogen bonds. (B) 3D model of the interaction between compound **6n** and tubulin. The protein is represented by molecular surface. **6n** is depicted by sticks and balls.

showed strong inhibitory effect and their 50% tubulin polymerization inhibition concentration of 9.2 μM and 4.3 μM.

2.4. Effects on cell cycle against cancer cells

To gain further insight into the action mode of these compounds, the most potent one was further assayed for their effects on cell cycle using flow cytometry (Fig. 2). As shown in Figure 2, compound **6n**, at low concentration (2 μg/mL), induced a practically complete cell cycle arrest at G2/M in B16-F10 cell. Over 70% of these cells were also arrested at G2/M after treatment with a 2 μg/mL concentration of **6n** for 24 h. These findings indicated a continuing impairment of cell division and confirmed compound **6n** was a potent antitubulin agent.

2.5. Molecular docking study of synthetic compounds

To help understand the SARs observed at the tubulin and guide further SAR studies, we proceeded to examine the interaction of compound **6n** with tubulin (PDB code: 1SA0). The molecular docking was performed by simulation of synthetic compounds into the colchicine binding site in tubulin. All docking runs were applied the Lamarckian genetic algorithm of Auto-Dock 4.0.28.[22]

2.5.1. Correlation between binding free energy and inhibitory activity

Table 2 lists the calculated binding free energies of oxadiazoline analogs with tubulin, and Figure 3 shows the relationship between the calculated binding free energies and the inhibitory activities, IC_{50} values. The multiple regression analysis (MRA)[23] was performed to explore whether the inhibitory potencies of oxadiazoline compounds could be correlated with the energetic data. The regression equation was obtained for the inhibitory potencies, $-\log IC_{50}$ values, represented as pIC_{50} values, using the total binding free energies, ΔG, as the sole descriptor variable. A good correlation was found between the inhibitory activities and the calculated binding free energies (Eq. 1), also shown in Figure 3. This relationship suggested the anti-proliferative effect was produced by direct connection of tubulin and the compound.

$$-\log IC_{50} = -0.1639 \times \Delta G + 1.5613 \quad (1)$$

$$(n = 20, R^2 = 0.71)$$

2.5.2. Binding model of compound 6n and tubulin

Molecular docking of the most potent inhibitor **6n** into the colchicine binding site of tubulin was performed on the binding model based on the tubulin structure (PDB code: 1SA0). The binding model of compound **6n** and tubulin is depicted in Figure 4A. In the binding model, compound **6n** is nicely bound to the colchicine site of tubulin via hydrogen bond with LYS 822 (angle N–H···O = 150.67, distance = 2.877 Å). The enzyme surface model was showed in Figures 4B, which revealed that the molecule was well embedded in the active pocket.

The binding model showed the importance of the oxadiazoline moiety, which performed as the hydrogen bond acceptor.

3. Conclusion

In summary, a series of oxadiazoline analogs **6a–6t** were designed, synthesized and evaluated for their biological activities. Among these compounds, **6n** showed the most potent antiproliferative activities against three cancer cells and demonstrated antitubulin polymerization activity (IC_{50} = 4.3 ± 0.7 μM), which was compared with the positive control (CA-4). Docking simulation was performed to position compound **6n** into the active site of tubulin (PDB ID: 1SA0) to determine the probable binding model. In summary, these oxadiazoline compounds substituted with naphthyl moiety show promising biological activity. Also detailed investigations are continuing to study the mechanisms of the inhibitory activity reported here.

4. Experimental section

4.1. Materials and measurements

All chemicals and reagents used in current study were of analytical grade. All the ^1H NMR spectra were recorded on a Bruker DPX 300 model spectrometer in $CDCl_3$ and chemical shifts were reported in ppm (δ). ESI-MS spectra were recorded on a Mariner System 5304 Mass spectrometer. Elemental analyses were performed on a CHN-O-Rapid instrument. TLC was performed on the glass-backed silica gel sheets (Silica Gel 60 GF254) and visualized in UV light (254 nm). Column chromatography was performed using silica gel (200–300 mesh) eluting with ethyl acetate and petroleum ether.

4.2. General procedure for the Preparation of target compounds 6a–6t

To a stirred solution of hydrazide **3** (1 mmol) and compound **4** (1 mmol) in ethanol (25 mL), water (5 mL) was added followed by dropwise addition of glacial acetic acid (0.2 mL). The resulting mixture was refluxed for 5 h, after which the solution was poured into ice water. The mixture was stirred until a precipitate formed,

which was collected using suction filtration and dried, followed by recrystallization in aqueous methanol.

Compounds **6** was synthesized by addition of acetic anhydride (2 mL) to hydrazone **5** (0.2 mmol), and the resulting solution was heated to reflux for 1 h. The reaction mixture was poured into ice water, and the resulting solid product was filtered and washed with copious amounts of water, drying under air.

4.2.1. 2-(2′-Naphthyl)-5-phenyl-2-acetyl-2,3-dihydro-1,3,4-oxadiazoline (6a)

Yield 67%; mp 148–151 °C. ^{1}H NMR ($CDCl_3$, 300 MHz): δ 8.34 (s, 1H), 7.98 (d, J = 9.0 Hz, 1H), 7.88 (t, J = 7.5 Hz, 3H), 7.51–7.58 (m, 4H), 7.40 (t, J = 3.45 Hz, 3H), 7.14 (s, 1H), 2.40 (s, 3H). MS (ESI): 317.12 ($C_{20}H_{17}N_2O_2$, $[M+H]^+$). Anal. Calcd for $C_{20}H_{16}N_2O_2$: C, 75.93; H, 5.10; N, 8.86. Found: C, 75.59; H, 5.19; N, 8.89.

4.2.2. 2-(2′-Naphthyl)-5-(4″-methoxyphenyl)-2-acetyl-2,3-dihydro-1,3,4-oxadiazoline (6b)

Yield 78%; mp 129–131 °C. ^{1}H NMR ($CDCl_3$, 300 MHz): δ 8.35 (s, 1H), 8.00 (d, J = 8.7 Hz, 1H), 7.91 (t, J = 9.0 Hz, 3H), 7.55–7.61 (m, 2H), 7.47 (d, J = 8.7 Hz, 2H), 7.11 (s, 1H), 6.94 (d, J = 8.7 Hz, 2H), 3.82 (s, 3H), 2.41 (s, 3H). MS (ESI): 347.13 ($C_{21}H_{19}N_2O_3$, $[M+H]^+$). Anal. Calcd for $C_{21}H_{18}N_2O_3$: C, 72.82; H, 5.24; N, 8.09. Found: C, 72.58; H, 5.20; N, 8.16.

4.2.3. 2-(2′-Naphthyl)-5-(2″-bromophenyl)-2-acetyl-2,3-dihydro-1,3,4-oxadiazoline (6c)

Yield 80%; mp 143–145 °C. ^{1}H NMR ($CDCl_3$, 300 MHz): δ 8.31 (s, 1H), 7.96 (d, J = 9 Hz, 1H), 7.84–7.88 (m, 3H), 7.65 (d, J = 7.8 Hz, 1H), 7.50–7.58 (m, 2H), 7.43 (s, 1H), 7.31–7.39 (m, 2H), 7.28 (s, 1H), 2.41 (s, 3H). MS (ESI): 395.04 ($C_{20}H_{16}BrN_2O_2$, $[M+H]^+$). Anal. Calcd for $C_{20}H_{15}BrN_2O_2$: C, 60.78; H, 3.83; N, 7.09. Found: C, 60.92; H, 3.90; N, 7.04.

4.2.4. 2-(2′-Naphthyl)-5-(3″-bromophenyl)-2-acetyl-2,3-dihydro-1,3,4-oxadiazoline (6d)

Yield 83%; mp 161–162 °C. ^{1}H NMR ($CDCl_3$, 300 MHz): δ 8.36 (s, 1H), 8.00 (d, J = 9 Hz, 1H), 7.90 (t, J = 15 Hz, 3H), 7.68 (d, 1H), 7.54–7.62 (m, 3H), 7.50 (d, J = 7.8 Hz, 1H), 7.32 (d, J = 7.5 Hz, 1H), 7.11 (s, 1H), 2.41 (s, 3H). MS (ESI): 395.08 ($C_{20}H_{16}BrN_2O_2$, $[M+H]^+$). Anal. Calcd for $C_{20}H_{15}BrN_2O_2$: C, 60.78; H, 3.83; N, 7.09. Found: C, 60.43; H, 3.85; N, 7.02.

4.2.5. 2-(2′-Naphthyl)-5-(4″-bromophenyl)-2-acetyl-2,3-dihydro-1,3,4-oxadiazoline (6e)

Yield 83%; mp 130–132 °C. ^{1}H NMR ($CDCl_3$, 300 MHz): δ 8.35 (s, 1H), 7.99 (d, J = 9.0 Hz, 1H), 7.90 (t, J = 9.0 Hz, 3H), 7.59 (m, 4H), 7.43 (d, J = 8.4 Hz, 2H), 7.11 (s, 1H), 2.41 (s, 3H). MS (ESI): 395.01 ($C_{20}H_{16}BrN_2O_2$, $[M+H]^+$). Anal. Calcd for $C_{20}H_{15}BrN_2O_2$: C, 60.78; H, 3.83; N, 7.09. Found: C, 60.11; H, 3.89; N, 7.14.

4.2.6. 2-(2′-Naphthyl)-5-(2″-chlorophenyl)-2-acetyl-2,3-dihydro-1,3,4-oxadiazoline (6f)

Yield 69%; mp 140–142 °C. ^{1}H NMR ($CDCl_3$, 300 MHz): δ 8.30 (s, 1H), 7.96 (d, J = 8.7 Hz, 1H), 7.86 (t, J = 14.0 Hz, 3H), 7.50–7.58 (m, 2H), 7.40–7.47 (m, 3H), 7.29–7.35 (m, 2H), 2.44 (s, 3H). MS (ESI): 351.09 ($C_{20}H_{16}ClN_2O_2$, $[M+H]^+$). Anal. Calcd for $C_{20}H_{15}ClN_2O_2$: C, 68.48; H, 4.31; N, 7.99. Found: C, 68.04; H, 4.35; N, 7.91.

4.2.7. 2-(2′-Naphthyl)-5-(4″-chlorophenyl)-2-acetyl-2,3-dihydro-1,3,4-oxadiazoline (6g)

Yield 75%; mp 148–150 °C. ^{1}H NMR ($CDCl_3$, 300 MHz): δ 8.33 (s, 1H), 7.96 (d, J = 9.0 Hz, 1H), 7.88 (t, J = 12.0 Hz, 3H), 7.54–7.60 (m, 2H), 7.46 (d, J = 9.0 Hz, 2H), 7.37 (d, J = 8.4 Hz, 2H), 7.1 (s, 1H), 2.39 (s, 3H). MS (ESI): 351.04 ($C_{20}H_{16}ClN_2O_2$, $[M+H]^+$). Anal. Calcd for $C_{20}H_{15}ClN_2O_2$: C, 68.48; H, 4.31; N, 7.99. Found: C, 68.91; H, 4.33; N, 7.95.

4.2.8. 2-(2′-Naphthyl)-5-(2″-fluorophenyl)-2-acetyl-2,3-dihydro-1,3,4-oxadiazoline (6h)

Yield 73%; mp 171–173 °C. ^{1}H NMR ($CDCl_3$, 300 MHz): δ 8.33 (s, 1H), 7.99 (d, J = 9 Hz, 1H), 7.89 (t, J = 13.5 Hz, 3H), 7.52–7.60 (m, 3H), 7.38–7.47 (m, 2H), 7.34 (s, 1H), 7.11–7.22 (m, 2H), 2.44 (s, 3H). MS (ESI): 335.19 ($C_{20}H_{16}FN_2O_2$, $[M+H]^+$). Anal. Calcd for $C_{20}H_{15}FN_2O_2$: C, 71.85; H, 4.52; N, 8.38. Found: C, 71.60; H, 4.61; N, 8.36.

4.2.9. 2-(2′-Naphthyl)-5-(3″-fluorophenyl)-2-acetyl-2,3-dihydro-1,3,4-oxadiazoline (6i)

Yield 85%; mp 170–171 °C. ^{1}H NMR ($CDCl_3$, 300 MHz): δ 8.33 (s, 1H), 8.00 (d, J = 8.6 Hz, 1H), 7.91 (t, J = 14.2 Hz, 3H), 7.54–7.62 (m, 3H), 7.35–7.44 (m, 2H), 7.26 (d, J = 13.5 Hz, 1H), 7.12 (d, J = 16 Hz, 2H), 2.43 (s, 3H). MS (ESI): 335.15 ($C_{20}H_{16}FN_2O_2$, $[M+H]^+$). Anal. Calcd for $C_{20}H_{15}FN_2O_2$: C, 71.85; H, 4.52; N, 8.38. Found: C, 71.71; H, 4.59; N, 8.46.

4.2.10. 2-(2′-Naphthyl)-5-(4″-fluorophenyl)-2-acetyl-2,3-dihydro-1,3,4-oxadiazoline (6j)

Yield 86%; mp 176–178 °C. ^{1}H NMR ($CDCl_3$, 300 MHz): δ 8.35 (s, 1H), 7.99 (d, J = 9 Hz, 1H), 7.90 (t, J = 15.0 Hz, 3H), 7.51–7.59 (m, 4H), 7.10 (t, J = 15.0 Hz, 3H), 2.41 (s, 3H). MS (ESI): 335.11 ($C_{20}H_{16}FN_2O_2$, $[M+H]^+$). Anal. Calcd for $C_{20}H_{15}FN_2O_2$: C, 71.85; H, 4.52 N, 8.38. Found: C, 71.23; H, 4.56; N, 8.45.

4.2.11. 2-(2′-Naphthyl)-5-(2″-nitrophenyl)-2-acetyl-2,3-dihydro-1,3,4-oxadiazoline (6k)

Yield 78%; mp 157–159 °C. ^{1}H NMR ($CDCl_3$, 300 MHz): δ 8.33 (s, 1H), 8.12 (d, J = 7.5 Hz, 1H), 7.94 (d, J = 9 Hz, 1H), 7.84–7.90 (m, 4H), 7.65 (d, J = 7.5 Hz, 1H), 7.51–7.57 (m, 4H), 2.46 (s, 3H). MS (ESI): 362.13 ($C_{20}H_{16}N_3O_4$, $[M+H]^+$). Anal. Calcd for $C_{20}H_{15}N_3O_4$: C, 66.48; H, 4.18; N, 11.63. Found: C, 66.97; H, 4.24; N, 11.54.

4.2.12. 2-(2′-Naphthyl)-5-(4″-nitrophenyl)-2-acetyl-2,3-dihydro-1,3,4-oxadiazoline (6l)

Yield 81%; mp 159–160 °C. ^{1}H NMR ($CDCl_3$, 300 MHz): δ 8.35 (s, 1H), 8.27 (d, J = 8.7 Hz, 2H), 7.98 (d, J = 9 Hz, 1H), 7.90 (t, J = 15.3 Hz, 3H), 7.73 (d, J = 8.8 Hz, 2H), 7.54–7.62 (m, 2H), 7.21 (s, 1H), 2.41 (s, 3H). MS (ESI): 362.11 ($C_{20}H_{16}N_3O_4$, $[M+H]^+$). Anal. Calcd for $C_{20}H_{15}N_3O_4$: C, 66.48; H, 4.18; N, 11.63. Found: C, 66.65; H, 4.22; N, 11.46.

4.2.13. 2-(2′-Naphthyl)-5-(2″-hydroxyphenyl)-2-acetyl-2,3-dihydro-1,3,4-oxadiazoline (6m)

Yield 55%; mp 137–139 °C. ^{1}H NMR ($CDCl_3$, 300 MHz): δ 8.30 (s, 1H), 7.96 (d, J = 8.7 Hz, 1H), 7.88 (d, J = 8.2 Hz, 3H), 7.50–7.59 (m, 3H), 7.44 (t, J = 14.0 Hz, 2H), 7.30 (d, J = 7.5 Hz, 1H), 7.20 (s, 1H), 7.17 (d, J = 8 Hz, 1H), 2.37 (s, 3H). MS (ESI): 333.13 ($C_{20}H_{17}N_2O_3$, $[M+H]^+$). Anal. Calcd for $C_{20}H_{16}N_2O_3$: C, 72.28; H, 4.85; N, 8.43. Found: C, 72.56; H, 4.73; N, 8.51.

4.2.14. 2-(2′-Naphthyl)-5-(2″-naphthyl)-2-acetyl-2,3-dihydro-1,3,4-oxadiazoline (6n)

Yield 71%; mp 166–167 °C. ^{1}H NMR ($CDCl_3$, 300 MHz): δ 8.28 (d, J = 8.4 Hz, 2H), 7.83–7.99 (m, 7H), 7.63 (t, J = 13.9 Hz, 1H), 7.48–7.57 (m, 5H), 2.51 (s, 3H). MS (ESI): 367.14 ($C_{24}H_{19}N_2O_2$, $[M+H]^+$). Anal. Calcd for $C_{24}H_{18}N_2O_2$: C, 78.67; H, 4.95; N, 7.65. Found: C, 78.89; H, 4.90; N, 7.74.

4.2.15. 2-(2′-Naphthyl)-5-(2″-pyridinyl)-2-acetyl-2,3-dihydro-1,3,4-oxadiazoline (6o)

Yield 62%; mp 142–145 °C. ^{1}H NMR ($CDCl_3$, 300 MHz): δ 8.68 (d, J = 4.8 Hz, 1H), 8.33 (s, 1H), 7.99 (d, J = 8.1 Hz, 1H), 7.87 (d, J = 11 Hz, 3H), 7.76 (t, J = 11 Hz, 1H), 7.49–7.58 (m, 3H), 7.32 (q, J = 12.6 Hz, 1H), 7.12 (s, 1H), 2.43 (s, 1H). MS (ESI): 318.11

($C_{19}H_{16}N_3O_2$, $[M+H]^+$). Anal. Calcd for $C_{19}H_{15}N_3O_2$: C, 71.91; H, 4.76; N, 13.24. Found: C, 72.28; H, 4.70; N, 13.15.

4.2.16. 2-(2′-Naphthyl)-5-(3″-pyridinyl)-2-acetyl-2,3-dihydro-1,3,4-oxadiazoline (6p)

Yield 67%; mp 140–142 °C. ^{1}H NMR ($CDCl_3$, 300 MHz): δ 8.82 (s, 1H), 8.66 (d, J = 3.6 Hz, 1H), 8.35 (s, 1H), 7.98 (d, J = 9 Hz, 1H), 7.84–7.91 (m, 4H), 7.53–7.61 (m, 2H), 7.36 (q, J = 12.6 Hz, 1H), 7.19 (s, 1H), 2.41 (s, 1H). MS (ESI): 318.15 ($C_{19}H_{16}N_3O_2$, $[M+H]^+$). Anal. Calcd for $C_{19}H_{15}N_3O_2$: C, 71.91; H, 4.76; N, 13.24. Found: C, 72.20; H, 4.79; N, 13.29.

4.2.17. 2-(2′-Naphthyl)-5-(4″-pyridinyl)-2-acetyl-2,3-dihydro-1,3,4-oxadiazoline (6q)

Yield 53%; mp 157–159 °C. ^{1}H NMR ($CDCl_3$, 300 MHz): δ 8.7 (d, J = 9.6 Hz, 2H), 8.37 (s, 1H), 7.89–8.0 (m, 4H), 7.55–7.64 (m, 2H), 7.49 (d, J = 4.2 Hz, 2H), 7.15 (s, 1H), 2.43 (s, 1H). MS (ESI): 318.14 ($C_{19}H_{16}N_3O_2$, $[M+H]^+$). Anal. Calcd for $C_{19}H_{15}N_3O_2$: C, 71.91; H, 4.76; N, 13.24. Found: C, 71.54; H, 4.70; N, 13.30.

4.2.18. 2-(2′-Naphthyl)-5-(4″-methyl)-2-acetyl-2,3-dihydro-1,3,4-oxadiazoline (6r)

Yield 73%; mp 157–159 °C. ^{1}H NMR ($CDCl_3$, 300 MHz): δ 8.33 (s, 1H), 7.98 (d, J = 6.9 Hz, 1H), 7.88 (d, J = 8.2 Hz, 3H), 7.53–7.59 (m, 2H), 7.41 (d, J = 8.3 Hz, 2H), 7.21 (d, J = 8.0 Hz, 2H), 7.10 (s, 1H), 2.44 (s, 1H). MS (ESI): 331.14 ($C_{21}H_{19}N_2O_2$, $[M+H]^+$). Anal. Calcd for $C_{21}H_{18}N_2O_2$: C, 76.34; H, 5.49; N, 8.48. Found: C, 76.73; H, 5.42; N, 8.55.

4.2.19. 2-(2′-Naphthyl)-5-(4″-thienyl)-2-acetyl-2,3-dihydro-1,3,4-oxadiazoline (6s)

Yield 67%; mp 148–152 °C. ^{1}H NMR ($CDCl_3$, 300 MHz): δ 9.97 (s, 1H), 9.28 (s, 1H), 8.92 (s, 1H), 8.37 (s, 1H), 7.89 (t, J = 14.6 Hz, 4H), 7.79 (q, J = 9.0 Hz, 2H), 1.53–7.62 (m, 2H), 7.24 (t, J = 8 Hz, 1H), 2.18 (s, 1H). MS (ESI): 325.09 ($C_{18}H_{17}N_2O_2S$, $[M+H]^+$). Anal. Calcd for $C_{18}H_{16}N_2O_2S$: C, 66.64; H, 4.97; N, 8.64. Found: C, 66.84; H, 4.94; N, 8.60.

4.2.20. 2-(2′-Naphthyl)-5-(4″-benzyloxyphenyl)-2-acetyl-2,3-dihydro-1,3,4-oxadiazoline (6t)

Yield 76%; mp 171–172 °C. ^{1}H NMR ($CDCl_3$, 300 MHz): δ 8.35 (s, 1H), 7.82–7.91 (m, 6H), 7.91 (t, J = 9.0 Hz, 3H), 7.57 (t, J = 7.5 Hz, 2H), 7.34–7.46 (m, 6H), 7.08 (d, J = 8.58 Hz, 2H), 5.15 (s, 2H), 2.16 (s, 3H). MS (ESI): 423.16 ($C_{27}H_{23}N_2O_3$, $[M+H]^+$). Anal. Calcd for $C_{27}H_{22}N_2O_3$: C, 76.76; H, 5.25; N, 6.63. Found: C, 76.32; H, 5.28; N, 6.53.

4.3. Antiproliferation assay

The antiproliferative activity of the prepared compounds against HepG2, MCF-7 and B16-F10 cells was evaluated as described elsewhere with some modifications.[24] Target tumor cell line was grown to log phase in RPMI 1640 medium supplemented with 10% fetal bovine serum. After diluting to 2×10^4 cells/mL with the complete medium, 100 μL of the obtained cell suspension was added to each well of 96-well culture plates. The subsequent incubation was permitted at 37 °C, 5% CO_2 atmosphere for 24 h before the cytotoxicity assessments. Tested samples at pre-set concentrations were added to 6-wells with colchicine and CSA-4 co-assayed as positive reference. After 48 h exposure period, 40 μL of PBS containing 2.5 mg/mL of MTT (3-(4,5-dimethylthiazol-2-yl)-2,5-diphenyltetrazolium bromide)) was added to each well. Four hours later, 100 μL extraction solution (10% SDS–5% isobutyl alcohol–0.01 M HCl) was added. After an overnight incubation at 37 °C, the optical density was measured at a wavelength of 570 nm on an ELISA microplate reader. In all experiments, three replicate wells were used for each drug concentration. Each assay was carried out at least three times. The results were summarized in Table 1.

4.4. Effects on tubulin polymerization

Bovine brain tubulin was purified as described previously.[25] To evaluate the effect of the compounds on tubulin assembly in vitro,[26] varying concentrations were preincubated with 10 μM tubulin in glutamate buffer at 30 °C and then cooled to 0 °C. After addition of GTP, the mixtures were transferred to 0 °C cuvettes in a recording spectrophotometer and warmed up to 30 °C and the assembly of tubulin was observed turbidimetrically. The IC_{50} was defined as the compound concentration that inhibited the extent of assembly by 50% after 20 min incubation.

4.5. Docking simulations

Molecular docking of synthetic compounds into the three-dimensional X-ray structure of *Escherichia* coli FabH (PDB code: 1SA0) was carried out using the AUTODOCK software package (version 4.0) as implemented through the graphical user interface AutoDock-Tools (ADT 1.4.6).[26]

The graphical user interface AUTODOCKTOOLS was employed to set-up the enzymes: all hydrogens were added, Gasteiger charges were calculated and nonpolar hydrogens were merged to carbon atoms. The Ni initial parameters are set as r = 1.170 Å, q = +2.0, and van der Waals well depth of 0.100 kcal/mol. For macromolecules, generated pdbqt files were saved.

The 3D structures of ligand molecules were built, optimized (PM3) level, and saved in Mol2 format with the aid of the molecular modeling program SPARTAN (Wavefunction Inc.). These partial charges of Mol2 files were further modified by using the ADT package (version 1.4.6) so that the charges of the nonpolar hydrogens atoms assigned to the atom to which the hydrogen is attached. The resultng files were saved as pdbqt files.

AUTODOCK 4.0 was employed for all docking calculations. The AUTODOCKTOOLS program was used to generate the docking input files. In all docking a grid box size of $60 \times 60 \times 60$ points in x, y, and z directions was built, the maps were centered on N1 atom of the Kcx 219 in the catalytic site of the protein. A grid spacing of 0.375 Å (approximately one forth of the length of carbon–carbon covalent bond) and a distances-dependent function of the dielectric constant were used for the calculation of the energetic map. Ten runs were generated by using Lamarckian genetic algorithm searches. Default settings were used with an initial population of 50 randomly placed individuals, a maximum number of 2.5×10^6 energy evaluations, and a maximum number of 2.7×10^4 generations. A mutation rate of 0.02 and a crossover rate of 0.8 were chosen. Results differing by less than 0.5 Å in positional root–mean–square deviation (RMSD) were clustered together and the results of the most favorable free energy of binding were selected as the resultant complex structures.

Acknowledgement

The work was financed by a grant (Project J1103512) from National Natural Science Foundation of China.

References and notes

1. Pettit, G. R.; Cragg, G. M.; Singh, S. B. *J. Nat. Prod.* **1987**, *50*, 386.
2. Pettit, G. R.; Singh, S. B.; Niven, M. L.; Hamel, E.; Schmidt, J. M. *J. Nat. Prod.* **1987**, *50*, 119.
3. Pettit, G. R.; Singh, S. B.; Hamel, E.; Lin, C. M.; Alberts, D. S.; Garcia-Kendall, D. *Experientia* **1989**, *45*, 209.
4. Lin, C. M.; Singh, S. B.; Chu, P. S.; Dempcy, R. O.; Schmidt, J. M.; Pettit, G. R.; Hamel, E. *Mol. Pharmacol.* **1988**, *34*, 200.

5. Ducki, S.; Forrest, R.; Hadfield, J. A.; Kendall, A.; Lawrence, N. J.; McGown, A. T.; Rennison, D. *Bioorg. Med. Chem. Lett.* **1998**, *8*, 1051.
6. Tron, G. C.; Pagliai, F.; Del Grosso, E.; Genazzani, A. A.; Sorba, G. *J. Med. Chem.* **2005**, *48*, 3260.
7. Wang, L.; Woods, K. W.; Li, Q.; Barr, K. J.; McCroskey, R. W.; Hannick, S. M.; Gherke, L.; Credo, R. B.; Hui, Y. H.; Marsh, K.; Warner, R.; Lee, J. Y.; Zielinski-Mozng, N.; Frost, D.; Rosenberg, S. H.; Sham, H. L. *J. Med. Chem.* **2002**, *45*, 1697.
8. Bailly, C.; Bal, C.; Barbier, P.; Combes, S.; Finet, J. P.; Hildebrand, M. P.; Peyrot, V.; Wattez, N. *J. Med. Chem.* **2003**, *46*, 5437.
9. Kim, Y.; Nam, N. H.; You, Y. J.; Ahn, B. Z. *Bioorg. Med. Chem. Lett.* **2002**, *12*, 719.
10. Nam, N. H.; Kim, Y.; You, Y. J.; Hong, D. H.; Kim, H. M.; Ahn, B. Z. *Bioorg. Med. Chem. Lett.* **2001**, *11*, 3073.
11. Nam, N. H.; Kim, Y.; You, Y. J.; Hong, D. H.; Kim, H. M.; Ahn, B. Z. *Bioorg. Med. Chem. Lett.* **2002**, *12*, 1955.
12. Simoni, D.; Grisolia, G.; Giannini, G.; Roberti, M.; Rondanin, R.; Piccagli, L.; Baruchello, R.; Rossi, M.; Romagnoli, R.; Invidiata, F. P.; Grimaudo, S.; Jung, M. K.; Hamel, E.; Gebbia, N.; Crosta, L.; Abbadessa, V.; Di Cristina, A.; Dusonchet, L.; Meli, M.; Tolomeo, M. *J. Med. Chem.* **2005**, *48*, 723.
13. Flynn, B. L.; Flynn, G. P.; Hamel, E.; Jung, M. K. *Bioorg. Med. Chem. Lett.* **2001**, *11*, 2341.
14. Gaukroger, K.; Hadfield, J. A.; Lawrence, N. J.; Nolan, S.; McGown, A. T. *Org. Biomol. Chem.* **2003**, *1*, 3033.
15. Gaukroger, K.; Hadfield, J. A.; Lawrence, N. J.; Nolan, S.; McGown, A. T. *Org. Biomol. Chem.* **2003**, *1*, 3033.
16. Tron, G. C.; Pirali, T.; Sorba, G.; Pagliai, F.; Busacca, S.; Genazzani, A. A. *J. Med. Chem.* **2006**, *49*, 3033.
17. Lee, L.; Robb, L. M.; Lee, M.; Davis, R.; Mackay, H.; Chavda, S.; Babu, B.; Orien, E. L.; Risinger, A. L.; Mooberry, S. L.; Lee, M. *J. Med. Chem.* **2009**, *53*, 325.
18. Kong, Y.; Grembecka, J.; Edler, M. C.; Hamel, E.; Mooberry, S. L.; Sabat, M.; Rieger, J.; Brown, M. L. *Chem. Biol.* **2005**, *12*, 1007.
19. Zhang, X.-M.; Qiu, M.; Sun, J.; Zhang, Y.-B.; Yang, Y.-S.; Wang, X.-L.; Tang, J.-F.; Zhu, H.-L. *Bioorg. Med. Chem.* **2011**, *19*, 6518.
20. Maya, A. B.; del Rey, B.; Lamamie de Clairac, R. P.; Caballero, E.; Barasoain, I.; Andreu, J. M.; Medarde, M. *Bioorg. Med. Chem. Lett.* **2000**, *10*, 2549.
21. Ali, O. M. A.; Abdel-Rahman, A. A.-H. *Synthesis* **2007**, *18*, 2823.
22. Huey, R.; Morris, G. M.; Olson, A. J.; Goodsell, D. S. *J. Comput. Chem.* **2007**, *28*, 1145.
23. Stahle, L.; Wold, S. *Prog. Med. Chem.* **1988**, *25*, 291.
24. Boumendjel, A.; Boccard, J.; Carrupt, P.-A.; Nicolle, E.; Blanc, M.; Geze, A.; Choisnard, L.; Wouessidjewe, D.; Matera, E.-L.; Dumontet, C. *J. Med. Chem.* **2008**, *51*, 2307.
25. Hamel, E.; Lin, C. M. *Biochemistry* **1984**, *23*, 4173.
26. Hamel, E. *Cell Biochem. Biophys.* **2003**, *38*, 1.